Eur. Phys. J. B **36**, 317–326 (2003)
DOI: 10.1140/epjb/e2003-00350-9

THE EUROPEAN PHYSICAL JOURNAL B

Selection rules and superconducting correlations in carbon nanotubes

J. González[a]

Instituto de Estructura de la Materia, Consejo Superior de Investigaciones Científicas, Serrano 123, 28006 Madrid, Spain

Received 13 August 2003
Published online 23 December 2003 – © EDP Sciences, Società Italiana di Fisica, Springer-Verlag 2003

Abstract. We carry out a detailed analysis of the effective interaction arising from electron-phonon scattering and its capability to produce the superconducting correlations observed in the carbon nanotubes. It is shown that certain selection rules prevent the exchange of phonons in some of the interaction channels, depending on the geometry of the nanotubes and on whether they are doped or not. In addition, we discuss the mechanism working in nanotube ropes by which the electrostatic coupling among a large number of metallic nanotubes leads to a substantial reduction in the strength of the Coulomb interaction. The scaling equation for the superconducting response function is then improved nonperturbatively, by including the exact contribution from forward-scattering processes. This allows us to estimate the boundary between superconducting and nonsuperconducting phases in the ropes, as well as to constrain the actual values of the strength of the effective attractive interaction.

PACS. 71.10.Pm Fermions in reduced dimensions (anyons, composite fermions, Luttinger liquid, etc.) – 73.63.Fg Nanotubes – 74.78.Na Mesoscopic and nanoscale systems

1 Introduction

During the last years there has been much activity devoted to study the transport properties of carbon nanotubes. The fact that they can show metallic or semiconducting behavior depending on the helicity of the tubule [1–3] makes them very suitable for the construction of devices in molecular electronics. Carbon nanotubes offer also an ideal ground to study the effects of electronic correlations, which are enhanced in systems with reduced dimensionality. In this respect, it has been paid attention mostly to situations where the dominant interaction is given by the Coulomb repulsion. It has been pointed out that the carbon nanotubes should be described then by the so-called Luttinger liquid behavior at large length scales, and that phases with broken symmetry could be only reached at extremely low energies [4,5].

The carbon nanotubes may display actually different behaviors in the transport measurements, depending essentially on the quality of the contacts attached to the nanotubes and the characteristic energy scale of the experiment. For contacts with very low transparency, genuine signatures of Luttinger liquid behavior can be observed in the power-law dependence of the conductance around room temperature [6,7]. At much lower energy scales, of the order of a few meV for nanotubes about 1 μm long, the effects of Coulomb blockade are present in the patterns of the conductance [8,9]. On the other hand, when the contacts with the electrodes have good quality, a completely different regime is measured in which the electrons may propagate ballistically along the nanotube [10,11]. In the case of nanotube ropes placed between superconducting contacts, it has been remarkable the observation of supercurrents that can flow over lengths of several microns, providing a clear signature of the superconducting proximity effect [12].

It is nowadays out of any doubt that certain nanotube samples may develop sensible superconducting correlations. The most favorable situation for their observation corresponds to the case of thick ropes which are long enough to maintain the coherence of the Cooper pairs. This can be concluded from all the experimental evidence that has been reported in reference [13]. In certain nanotube ropes, a drop of several orders of magnitude in the resistance has been measured, showing the onset of a superconducting transition in the system with a finite number of channels [14]. Strong superconducting correlations have been also measured in nanotubes of very small radius $R \approx 0.2$ nm, inserted in a zeolite matrix [15]. In that kind of experiment, the effects studied have one-dimensional (1D) character, but clear superconductivity features have been obtained from the tendency to expel the magnetic flux and the divergent behavior of the conductance.

The observation of superconducting correlations implies the existence of an attractive component of the interaction in the carbon nanotubes. The analyses of the electron correlations in the tubules have shown that it is not

[a] e-mail: imtjg64@pinar2.csic.es

plausible the opening of an attractive channel arising from the purely repulsive Coulomb interaction, at least without going down to extremely low energies [4,5]. Then, it is most likely that the attractive interaction comes from the coupling to the elastic modes of the nanotube lattice [16]. It remains the question of how the large Coulomb repulsion present in the nanotubes may be overcome by the attraction due to the phonon exchange. By means of a simple estimate, it can be seen that the strength of the latter is much smaller than the nominal strength of the Coulomb interaction, for nanotubes with the typical radii found in the ropes. It has been shown, however, that the electrostatic coupling between a large number of metallic nanotubes leads to a substantial reduction of the repulsive interaction within each nanotube [17,18]. This would explain why the superconducting correlations develop preferently in ropes with a large content of metallic nanotubes.

The purpose of the present paper is to accomplish a detailed analysis of the effective interaction arising from electron-phonon scattering and its capability to produce the superconducting correlations in the carbon nanotubes. Previous investigations have focused on the properties of the armchair nanotubes [18]. We will pay attention here to armchair and zigzag geometries, discerning the cases of doped and undoped nanotubes. Certain selection rules for the electron-phonon couplings can be shown to arise, preventing the exchange of phonons in some of the channels for each particular instance. This has a direct impact on the strength of the superconducting correlations, which turns out to depend on the geometry of the nanotubes and whether they are doped or not.

We will carry out our analysis having in mind the physical parameters appropriate for the carbon nanotubes found in the ropes. This will lead us to consider a strength of the effective attractive interaction which corresponds to the weak-coupling regime. We will see that, for sufficiently large number of metallic nanotubes in a rope, the electron system falls in a phase where the superconducting correlations grow large at low energies. This is consistent with the experimental results that have been reported recently in reference [13]. The evidence found from measurements in a number of different samples is that the correlations are able to drive to a superconducting transition only above a certain content of metallic nanotubes in the rope. This information will allow us to estimate the boundary between superconducting and nonsuperconducting phases in the ropes, as well as to constrain the actual values of the strength of the effective attractive interaction.

The content of this paper is distributed as follows. In the next section we discuss the effect of phonon exchange and the selection rules that apply to different electron-phonon scattering processes. Section 3 is devoted to set up the framework to study the competition between the repulsive Coulomb interaction and the effective interaction arising from phonon exchange. In Section 4, we establish the conditions that make possible the growth of the superconducting correlations, identifying the superconducting phase in the diagram for the nanotube ropes. Finally, the conclusions of our study are drawn in Section 5.

2 Effective interactions and selection rules from electron-phonon scattering

The electrons couple to the phonons of the nanotube lattice, and this gives rise to an effective electron-electron interaction that may be attractive in some instances. The interaction is retarded due to the phonon propagation between the two scattered electrons. This can be represented in terms of an effective potential $V(\omega)$ depending on the frequency ω [19]

$$V(\omega) = -g(k,k')g(q,q')\frac{\omega_{k-k'}}{-\omega^2+\omega_{k-k'}^2} \qquad (1)$$

$\omega_{k-k'}$ being the energy of the phonon with momentum $k-k'$ and $g(k,k')$ the appropriate electron-phonon couplings (defined below).

We observe from equation (1) that the effective interaction becomes attractive at frequencies below the scale of the phonon energy ω_k. This means that the high-energy phonons should play the most important role in the development of superconducting correlations in the nanotubes. In this respect, most part of the acoustic phonons have a dispersion relation with a linear dependence $\omega_k \approx v_s|k|$ at small momentum [20], which does not lead to a significant range of attraction for the effective interaction. A detailed study of the effect of acoustic phonons in a 1D system has been carried out in reference [21], taking into account the retardation of the interaction. It has been shown there that, although the exchange of acoustic phonons may lead to superconducting correlations in the 1D system, these are in general very weak since the critical exponents deviate from the noninteracting behavior by corrections of the order of $(v_s/v_F)^2$, v_F being the Fermi velocity in the electron system. Given that the sound velocity v_s for a linear phonon branch is more than 40 times smaller than the Fermi velocity v_F, we see that the influence of the acoustic phonons is negligible regarding the superconducting effects in carbon nanotubes.

The above argument applies to the acoustic branches with linear dispersion, and it also allows to neglect the effects of the mode corresponding to bending motion, with quadratic dispersion relation. The rest of acoustic modes have a finite energy at zero momentum, of the order of 10^{-2} eV [20], and such a small magnitude also implies important retardation effects. This is the case of the breathing mode in carbon nanotubes with the radii typically found in ropes, around 0.7 nm. One has to bear in mind, however, that the characteristic energy of that mode is inversely proportional to the nanotube radius, so that it could lead to an attractive interaction in a significant range of energies for nanotubes with very small radius R around 0.2 nm, as pointed out in reference [22].

We turn then our attention to the high-energy phonons, i.e. optical phonons at the top of the spectrum, which have an energy around 0.2 eV [23–25]. We focus on the evaluation of the electron-phonon couplings, which dictate the strength of the effective interaction in (1). We will represent them as $g_{p,p'}(k,k')$, showing explicitly the dependence on the respective subbands p and p' to which

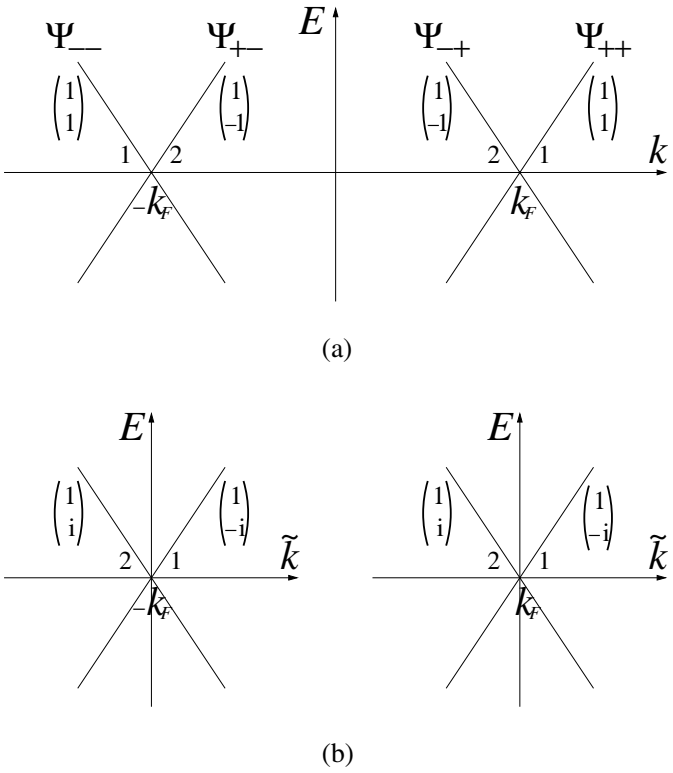

Fig. 1. Linear branches in the low-energy electronic spectrum of armchair nanotubes (upper diagram) and zigzag nanotubes (lower diagram). The eigenvectors representing the relative electron amplitudes in the two atoms of the lattice basis are given near each linear branch. The labels 1 and 2 denote the subband to which the linear branch belongs, according to the symmetry of the eigenvector.

the *in* and *out* electron modes belong. This notation is quite convenient, since the low-energy modes fall into two different gapless subbands, which may be distinguished by the different symmetry of the electron amplitudes in the two-atom basis of the nanotube lattice.

We recall that the low-energy electronic spectrum of a metallic nanotube is given by two pairs of linear branches crossing at opposite points in momentum space, as shown in Figure 1. For armchair nanotubes, the vector connecting the two points can be taken along the direction of the tubule axis [3]. The linear branches correspond then to the different eigenvalues of a one-particle Hamiltonian operating in the two-atom basis of the lattice [26], given by

$$\mathcal{H} \approx \pm \begin{pmatrix} 0 & \tilde{k} \\ \tilde{k} & 0 \end{pmatrix} \tag{2}$$

where the upper (lower) sign applies to the right (left) crossing point, with respect to which the momentum $\tilde{k}$ is measured in each case. We find therefore that the electron modes fall into bonding and antibonding subbands, represented respectively by the outer and inner branches in the upper diagram of Figure 1.

For the zigzag nanotubes, the vector connecting the two points where the linear branches meet is transverse to the longitudinal direction of the tubule [3]. The low-energy modes near each crossing point correspond to the different eigenvalues of the one-particle Hamiltonian [26]

$$\mathcal{H} \approx \begin{pmatrix} 0 & i\tilde{k} \\ -i\tilde{k} & 0 \end{pmatrix} \tag{3}$$

where $\tilde{k}$ represents the longitudinal momentum. As well as for the Hamiltonian in (2), the eigenvectors of (3) bind the relative electron amplitudes in the two atoms of the lattice basis. The different symmetry of the eigenvectors depending on the particular linear branch of the zigzag nanotube is represented in the lower diagram of Figure 1.

The optical phonons correspond to localized displacements of the nanotube lattice, what makes appropriate the use of a tight-binding approximation for the calculation of the electron-phonon couplings [27]. These depend on the amplitudes of the electron modes, obtained in general from the eigenvectors of (2) and (3) times a plane-wave factor, and which we write as $u_s^{(p)}(k)$, where the index s stands for the lattice site. The electron-phonon couplings can be represented by a sum over nearest neighbors of the atoms in the unit cell of the nanotube [28]

$$g_{p,p'}(k,k') = \frac{1}{(\mu\ \omega_{k-k'})^{1/2}} \times \sum_{\langle s,s' \rangle} u_s^{(p)*}(k) u_{s'}^{(p')}(k') (\boldsymbol{\epsilon}_s(k-k') - \boldsymbol{\epsilon}_{s'}(k-k')) \cdot \boldsymbol{\nabla} J(s,s') \tag{4}$$

where $\boldsymbol{\epsilon}_s(k-k')$ is the phonon polarization vector at site s, $J(s,s')$ is the matrix element of the potential between orbitals at s and s', and μ is the mass per unit length.

The tight-binding approximation has been used in reference [28] in the computation of the electron-phonon couplings involving acoustic phonons in the armchair nanotubes. It has been noticed that certain constraints arise in the emission or absorption of phonons, which depend on their particular polarization. The relations that exist between the couplings for different subbands p and p' can be extended to the case of the optical phonons, and for any kind of metallic nanotube [18]. Thus, it turns out that, in general,

$$g_{1,1}(k,k') = -g_{2,2}(k,k') \tag{5}$$

$$g_{1,2}(k,k') = -g_{2,1}(k,k'). \tag{6}$$

It can be also shown that the electron-phonon couplings vanish for special kinematics. This can be observed in the explicit expressions obtained in reference [28] for acoustic phonons in the armchair nanotubes. We study in what follows the selection rules that apply in the armchair and the zigzag nanotubes, for optical as well as for acoustic phonons.

We first show that, in the armchair nanotubes, the amplitude for phonon emission or absorption vanishes when the *in* and *out* electron modes are in different subbands and have opposite momenta:

$$g_{1,2}(k,-k) = 0. \tag{7}$$

This can be seen by inspection of the formula (4), noticing that one of the electron modes in each term of the sum must have the lower amplitude of an eigenvector of (2), while the other must have the upper amplitude (since the points s and s' belong to different nanotube sublattices). If the latter mode belongs to the antibonding subband, the former belongs to the bonding subband, and we have a contribution to the sum in (4) of the form

$$e^{-ikx_s}e^{-ikx_{s'}}(\boldsymbol{\epsilon}_s(2k)-\boldsymbol{\epsilon}_{s'}(2k))\cdot\boldsymbol{\nabla}J(s,s') \qquad (8)$$

where we denote by x_s the position of the site s along the nanotube. We can however reverse the order in which we take the points s and s' in the sum. In that case, the mode in the antibonding subband gets the lower amplitude of the eigenvector, and we have a contribution to the coupling

$$-e^{-ikx_{s'}}e^{-ikx_s}(\boldsymbol{\epsilon}_{s'}(2k)-\boldsymbol{\epsilon}_s(2k))\cdot\boldsymbol{\nabla}J(s',s). \qquad (9)$$

The two contributions (8) and (9) are opposite, what shows that the terms in (4) cancel out in pairs, when the incoming and outgoing electrons are in different subbands with opposite momenta (for armchair nanotubes).

Shifting now to the case of the zigzag nanotubes, one can show that the electron-phonon coupling vanishes when the electron reverses its momentum in the scattering process, but remaining now within the same subband:

$$g_{1,1}(k,-k)=g_{2,2}(k,-k)=0. \qquad (10)$$

This can be seen using the expression of the eigenvectors of (3) for a zigzag nanotube, which have a lower amplitude equal to i or $-i$ when the upper amplitude is chosen equal to 1. Let us consider the subband corresponding to the first instance, as the other is completely equivalent. Then, for a given term of the sum in (4), if the *in* mode has the upper amplitude 1, the *out* mode must have the lower amplitude i (since the points s and s' belong to different nanotube sublattices). We have a contribution of the form

$$-ie^{-i\tilde{k}x_s}e^{-ik_Fy_s}e^{-i\tilde{k}x_{s'}}e^{-ik_Fy_{s'}}\big(\boldsymbol{\epsilon}_s(2\tilde{k}+2k_F) - \boldsymbol{\epsilon}_{s'}(2\tilde{k}+2k_F)\big)\cdot\boldsymbol{\nabla}J(s,s'). \qquad (11)$$

In this expression, we have supposed that the momentum k decomposes into the longitudinal component $\tilde{k}$ and the large transverse momentum k_F of the Fermi point (for the undoped system), while y_s denotes the position along the tangential direction of the nanotube. We compare again with the term in which the lattice sites s and s' have been exchanged. In that case, the *in* mode has the lower amplitude in the two-atom basis, and the *out* mode gets the relative amplitude equal to 1, giving rise to a contribution

$$ie^{-i\tilde{k}x_{s'}}e^{-ik_Fy_{s'}}e^{-i\tilde{k}x_s}e^{-ik_Fy_s}\big(\boldsymbol{\epsilon}_{s'}(2\tilde{k}+2k_F) - \boldsymbol{\epsilon}_s(2\tilde{k}+2k_F)\big)\cdot\boldsymbol{\nabla}J(s',s). \qquad (12)$$

The two contributions in (11) and (12) differ by a minus sign. The argument allows then to conclude that the terms in (4) cancel out in pairs when the incoming and outgoing electrons are in the same subband with opposite momenta (for zigzag nanotubes).

The large momentum of the Fermi point does not play a significant role in the above argument, and it can be shown actually that the selection rule holds also when the *in* and *out* modes have opposite longitudinal momenta *about the same* crossing point at k_F or $-k_F$. In this case, there is a variation in the argument in that, if the term corresponding to (11) has now the factor $e^{ik_Fy_s}e^{-ik_Fy_{s'}}$, the term obtained by exchanging s and s' contains instead the factor $e^{ik_Fy_{s'}}e^{-ik_Fy_s}$. We have to bear in mind, though, that each atom in the zigzag nanotubes has two nearest neighbors with equal longitudinal coordinate x_s and opposite tangential coordinate y_s relative to that of the given atom. Thus, combining the respective terms in the sum (4), we end up with contributions which contain the factor $\cos(ik_F(y_s-y_{s'}))$ and whose only difference upon the exchange of x_s and $x_{s'}$ is the relative minus sign as in (11) and (12). We conclude that the selection rule (10) also holds for scattering processes where the longitudinal component of the momentum is reversed around a given crossing point at k_F or $-k_F$.

The selection rule (10) is actually the consequence of a more general rule in the zigzag nanotubes. We can state it by saying that two electron-phonon scattering processes with the same momentum transfer may have opposite amplitudes, if the momenta of the electrons lie in the respective processes at opposite sides of the given crossing point at k_F or $-k_F$. By means of the same argument applied above, one can easily see, for instance, that

$$g_{1,1}(-k,0)=-g_{1,1}(0,k) \qquad (13)$$

$$g_{2,2}(-k,0)=-g_{2,2}(0,k). \qquad (14)$$

The electron-phonon couplings $g_{1,1}(k,k')$ and $g_{2,2}(k,k')$ are actually odd functions of the sum of the incoming and outgoing longitudinal momenta in the zigzag nanotubes. A similar property may be observed in the explicit computation of the $g_{1,2}(k,k')$ coupling in the armchair nanotubes [28]. The odd character of the couplings acquires great significance when the nanotubes are not doped. In that case, the electrons are scattered near k_F or $-k_F$, and we are led to conclude that the electron-phonon scattering amplitudes involving the couplings with alternating sign must average to zero. This has in turn important consequences for the effective interaction mediated by phonons, as we will see in what follows.

3 Coulomb versus phonon-exchange interactions in carbon nanotubes

We now study the conditions under which the effective interaction coming from phonon exchange may balance the repulsive Coulomb interaction in the carbon nanotubes. In this respect, we discuss here a mechanism working in nanotube ropes, according to which the electrostatic coupling among a large number of metallic nanotubes leads

to a substantial reduction in the strength of the Coulomb interaction [18]. We assume that the long-range character of the latter gives rise to the coupling between charges in different metallic nanotubes of a rope. The Coulomb potential projected onto the longitudinal dimension of the nanotubes takes the form [29]

$$V_C(k) = (e^2/2\pi)\log|(k_c + k)/k| \tag{15}$$

where k is the longitudinal component of the momentum and k_c, of the order of $\sim 1/R$, is the memory that the potential keeps of the finite radius of the nanotube [4]. The logarithmic dependence of the potential (15) at small momentum transfer is a feature of the long-range interaction, which remains unscreened in a 1D electron system with a finite number of interaction channels [30,31].

It has been shown that the backscattering and Umklapp processes mediated by the Coulomb interaction are highly suppressed in the carbon nanotubes [4,5]. Their amplitude turns out to be reduced by a factor of the order of $\sim 0.1a/R$ (a being the C-C distance) with respect to the nominal strength of the Coulomb interaction. The competition between that and the effective interaction from phonon exchange takes place mainly in processes involving the interaction of electronic currents in well-defined linear branches. For this reason, we take as starting point a model in which the elementary objects are the corresponding electron density operators. These can be expressed in terms of the Fermi fields $\Psi^{(a)}_{ri\sigma}(x)$ shown in Figure 1 for the different linear branches:

$$\Psi^{(a)\dagger}_{ri\sigma}(x)\Psi^{(a)}_{ri\sigma}(x) = \rho^{(a)}_{ri\sigma}(x). \tag{16}$$

The label a runs over the different metallic nanotubes in a rope, $a = 1, \ldots n$. The index $r = \pm$ is used to label the left- or right-moving character of the linear branch, and the index $i = \pm$ to label the Fermi point. The index σ stands for the two different spin projections.

The Coulomb interaction acts between any two density operators in (16) with a strength given by the potential (15). We may carry out the discussion in terms of the charge density operators $\rho^{(a)}_{ri\rho}(k)$, formed by the symmetric combination of density operators for the two spin projections

$$\rho^{(a)}_{ri\rho}(k) = \frac{1}{\sqrt{2}}\left(\rho^{(a)}_{ri\uparrow}(k) + \rho^{(a)}_{ri\downarrow}(k)\right). \tag{17}$$

Moreover, it is convenient to define the combinations

$$\tilde{\rho}^{(a)}_{1\rho}(k) = \rho^{(a)}_{++\rho}(k) + \rho^{(a)}_{--\rho}(k) \tag{18}$$

$$\tilde{\rho}^{(a)}_{2\rho}(k) = \rho^{(a)}_{+-\rho}(k) + \rho^{(a)}_{-+\rho}(k). \tag{19}$$

Regarding the interaction processes mediated by phonons, we have to specialize to each particular nanotube geometry. In the case of the armchair nanotubes, we have that the exchange of phonons gives rise to a repulsive interaction between currents in different subbands, according to the minus sign in equation (5). Thus, if we define

$$\tilde{\rho}^{(a)}_{+\rho}(k) = \frac{1}{\sqrt{2}}\left(\tilde{\rho}^{(a)}_{1\rho}(k) + \tilde{\rho}^{(a)}_{2\rho}(k)\right) \tag{20}$$

$$\tilde{\rho}^{(a)}_{-\rho}(k) = \frac{1}{\sqrt{2}}\left(\tilde{\rho}^{(a)}_{1\rho}(k) - \tilde{\rho}^{(a)}_{2\rho}(k)\right) \tag{21}$$

the effective interaction mediated by phonons involves the antisymmetric combinations $\tilde{\rho}^{(a)}_{-\rho}(k)$, which incorporate the relative minus sign that appears when coupling the two different subbands. We can write then the integrable part of the Hamiltonian containing just the forward-scattering processes in the form

$$\begin{aligned} H_{FS} = {} & \frac{1}{2}v_F\int_{-k_c}^{k_c} dk \sum_{ari\sigma} :\rho^{(a)}_{ri\sigma}(k)\rho^{(a)}_{ri\sigma}(-k): \\ & + \frac{1}{2}\int_{-k_c}^{k_c}\frac{dk}{2\pi}\left(4\sum_a \tilde{\rho}^{(a)}_{+\rho}(k)\, V_C(k) \sum_b \tilde{\rho}^{(b)}_{+\rho}(-k)\right. \\ & \left. +4g\sum_a \tilde{\rho}^{(a)}_{-\rho}(k)\, \tilde{\rho}^{(a)}_{-\rho}(-k)\right) \end{aligned} \tag{22}$$

where $g(<0)$ is the coupling that parameterizes the strength of the phonon mediated interaction at small momentum transfer.

We recall that the amplitude for single-electron tunneling between neighboring metallic nanotubes in a disordered rope has to be highly suppressed, due to the mismatch that exists in general in the orientation of the respective lattices [32]. This has been confirmed in the experiments reported in reference [33], where the coupling resistance between tubes in a rope has shown to be about three orders of magnitude above the typical resistance of metallic nanotubes. It is justified then the approximation made by taking for the kinetic term in (22) the sum of the kinetic terms of the individual metallic nanotubes,

In the case of the undoped zigzag nanotubes, we have to take into account the selection rules from equation (10). These have a significant effect when the Fermi level is at the crossing point of the linear branches. Although the longitudinal momentum of a scattered electron may not be exactly reversed by phonon emission or absorption, the amplitude is largely suppressed for processes in which the electron is promoted within the same subband from below to above the Fermi level, or vice versa. Actually, these processes average to zero, since the electron-phonon coupling is an odd function of the sum of the longitudinal momenta for the *in* and *out* modes, as shown in the preceding section. Thus, for undoped zigzag nanotubes, the influence of the phonon exchange is not significant in forward-scattering interactions. This does not mean that the Coulomb interaction has to be necessarily dominant in that instance since, as we will see, there is still an important backscattering interaction mediated by phonons that may trigger the superconducting correlations.

In the case of doped zigzag nanotubes, the most likely situation is that both the *in* and *out* electron modes lie below or above the point where the linear branches meet,

depending on the position of the Fermi level. Therefore, the selection rules in equation (10) are not relevant in this case. There is however a difference with respect to the previous description for the armchair nanotubes. It can be seen that the interaction mediated by phonons between a left-moving and a right-moving current is now always attractive. This follows from the complex conjugate relation that exists between the linear branches with opposite chirality, as shown in Figure 1, and that extends to the electron-phonon couplings with opposite momentum transfer appearing in (1). On the other hand, currents with the same right- or left-moving character belong to the same subband, and their interaction by phonon exchange has to be also attractive. The Hamiltonian for the integrable forward-scattering interactions in the doped zigzag nanotubes can be written in the form

$$H_{FS} = \frac{1}{2} v_F \int_{-k_c}^{k_c} dk \sum_{ari\sigma} : \rho_{ri\sigma}^{(a)}(k) \rho_{ri\sigma}^{(a)}(-k) : + \frac{1}{2} \int_{-k_c}^{k_c} \frac{dk}{2\pi} \left(4 \sum_a \tilde{\rho}_{+\rho}^{(a)}(k)\, V_C(k) \sum_b \tilde{\rho}_{+\rho}^{(b)}(-k) + 4g \sum_a \tilde{\rho}_{+\rho}^{(a)}(k)\, \tilde{\rho}_{+\rho}^{(a)}(-k) \right). \quad (23)$$

An important fact regarding the Coulomb interaction is that, as can be appreciated in (22) and (23), it operates on the total charge density for all the metallic nanotubes of the rope. Both Hamiltonians can be diagonalized by changing to a set of variables given by the totally symmetric combination of the $\tilde{\rho}_{+\rho}^{(a)}(k)$ operators, plus $n-1$ antisymmetric combinations of them suitably defined to make orthogonal the new variables. Thus, the Coulomb interaction only acts in one of the $4n$ possible interaction channels in a rope with n metallic nanotubes. That explains why its effect is less significant in the nanotube ropes as the number of metallic nanotubes increases. In the absence of real screening of the long-range interaction, the substantial reduction in the strength of the Coulomb repulsion is the relevant effect in thick nanotube ropes, arising as a consequence of the electrostatic coupling of the charges in the different metallic nanotubes.

4 Superconducting correlations in carbon nanotubes

We determine now the conditions under which the superconducting correlations grow large in the carbon nanotubes. For this purpose, one has to study the appropriate response functions $R(k,\omega)$, which are given by correlators of the operators $\mathcal{O}(k,\omega)$ representing the order parameters for the condensation of the Cooper pairs:

$$R(q,\omega) = \left\langle \mathcal{O}(q,\omega) \mathcal{O}^{\dagger}(q,\omega) \right\rangle . \quad (24)$$

We will deal with the formation of Cooper pairs with zero total momentum, so that we will stick to the case $q=0$ in the above definition.

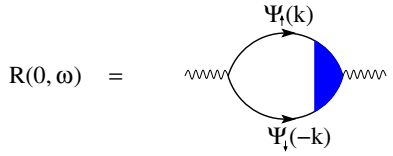

Fig. 2. Diagrammatic representation of the response function corresponding to a superconducting order parameter. The dark sector stands for the full vertex and the fermion lines represent the full electron propagators.

The operators reflecting the s-wave and p-wave symmetry of the Cooper pairs correspond respectively to the upper and lower signs in the following combination:

$$\mathcal{O}(0,\omega) = \sum_k \left(\Psi_{++\uparrow}(k)\Psi_{--\downarrow}(-k) \mp \Psi_{++\downarrow}(k)\Psi_{--\uparrow}(-k) + \Psi_{-+\uparrow}(k)\Psi_{+-\downarrow}(-k) \mp \Psi_{-+\downarrow}(k)\Psi_{+-\uparrow}(-k) \right). \quad (25)$$

The existence of four low-energy branches in the nanotubes allows in principle for more exotic possibilities, and we can have for instance an operator representing an order parameter with "d-wave" symmetry:

$$\mathcal{O}(0,\omega) = \sum_k \left(\Psi_{++\uparrow}(k)\Psi_{--\downarrow}(-k) - \Psi_{++\downarrow}(k)\Psi_{--\uparrow}(-k) - \left(\Psi_{-+\uparrow}(k)\Psi_{+-\downarrow}(-k) - \Psi_{-+\downarrow}(k)\Psi_{+-\uparrow}(-k) \right) \right). \quad (26)$$

For the evaluation of the response functions at low frequencies, we first resort to a perturbative renormalization group approach. It is known that the derivative of each response function

$$\overline{R}(\omega) = \frac{\partial R(0,\omega)}{\partial \log \omega} \quad (27)$$

is bound to satisfy a scaling equation [34], which dictates the power-law behavior of the response function at small ω. The anomalous exponent for that behavior can be obtained in perturbation theory by looking at the diagrammatic representation of $R(0,\omega)$. This is given in general by a closed equation of the type represented in Figure 2 [34].

The terms obtained by expansion of the diagram in Figure 2 depend actually on the high-energy cutoff $E_c = v_F k_c$, which can be used to derive the scaling equation for $\overline{R}(\omega)$. The technique commonly applied consists in differentiating the response function with respect to E_c, with the aim of trading later this dependence by that on ω in the functions with perfect scaling behavior [35].

The first perturbative orders of the response function are formed through interaction processes in which a pair of *in* electron modes to the left of the diagram in Figure 2 are scattered into a pair of *out* electron modes to the right. We will follow here the convention of classifying the four-fermion interactions into different channels with respective coupling constants $g_i^{(j)}$ [36]. The lower index discerns whether the interacting particles shift from one Fermi point to the other ($i=1$), remain at different Fermi points ($i=2$), or they interact near the same

Fermi point ($i = 4$). The upper label follows the same rule to classify the different combinations of left-movers and right-movers, including the possibility of having Umklapp processes ($j = 3$).

We observe that four different types of processes arise to first order in the perturbative expansion of $R(0, \omega)$. Accordingly, the scaling equation for $\overline{R}(\omega)$ corresponding to s-wave or p-wave symmetry turns out to be

$$E_c \frac{\partial \log \overline{R}(\omega)}{\partial E_c} = -\frac{1}{\pi v_F} \left(g_2^{(2)} \pm g_1^{(1)} + g_2^{(1)} \pm g_1^{(2)} \right) + O\left(\left(g_i^{(j)} \right)^2 \right) \quad (28)$$

where the upper sign holds for singlet pairing and the lower sign for triplet pairing. We remark that the interactions mediated by phonons give negative contributions to all of the four couplings that appear at the r.h.s. of equation (28) [18]. This goes in the direction of strengthening the s-wave response function at large values of the cutoff E_c or, equivalently, at small values of the frequency ω. Consequently, only the development of superconducting correlations with the s-wave symmetry is plausible, at least in the weak-coupling regime of the phonon-mediated interaction.

The Coulomb repulsion provides anyhow a large positive contribution to $g_2^{(2)}$, that we can estimate as

$$v \approx (e^2/2\pi) \log |k_c/k_0| \quad (29)$$

taking an average momentum $k_0 \sim 10^{-3} k_c$ in the infrared, which is appropriate for nanotubes with a length of a few microns. We assume that a reasonable value of the coupling for the repulsive interaction in the nanotubes (with an implicit dielectric constant) is given by $e^2/\pi^2 v_F \approx 0.5$. On the other hand, for the scattering processes relevant for superconductivity, the values of the potential in (1) can be estimated in terms of the variation of the matrix element J with the C-C distance, given by $\partial J/\partial a \approx 4.5$ eVÅ^{-1}, and the typical Debye frequency ω_D of the phonons, in the range between 0.1 and 0.2 eV. Comparing with the Fermi velocity v_F in the carbon nanotubes, we find that $|g| \sim (\partial J/\partial a)^2/\mu\omega_D^2 \sim 0.1 v_F$. It turns out that, for individual nanotubes with a typical radius around 0.7 nm, the contribution to the r.h.s. of (28) from the phonon-mediated interaction cannot overcome the effect of the repulsive interaction.

In nanotube ropes, however, we can compute the exact contribution to the anomalous dimension in (28) from the forward-scattering interactions, finding out that the effective attractive interaction prevails for sufficiently large number n of metallic nanotubes. We improve then the perturbative equation (28) replacing the term $g_2^{(2)}$ at the r.h.s. by the nonperturbative contribution obtained from the model developed in the preceding section. In this procedure, we should differentiate between superconducting correlations in an armchair or a zigzag nanotube. Moreover, we have to distinguish between the cases of doped and undoped nanotube ropes. In order to simplify the computation, we will consider $R(0, \omega)$ for an armchair nanotube in the hypothetical case that the metallic nanotubes in the rope are armchair, and for a zigzag nanotube assuming that the metallic nanotubes in the rope are zigzag as well. This is justified since the choice of a particular environment of metallic nanotubes does not have a significant influence on the effect of the electrostatic coupling between them, while $R(0, \omega)$ depends essentially on the geometry and doping level of the nanotube in which it is computed.

We first consider the case of undoped armchair nanotubes. The anomalous dimension γ of the propagator for the Cooper pairs in the model with Hamiltonian (22) has been computed in reference [18], with the result that

$$\gamma = \frac{1}{2} - \frac{1}{2}\sqrt{1 - 4|g|/\pi v_F} + \frac{1}{2n} - \frac{1}{2n}\sqrt{1 + 4nv/\pi v_F}. \quad (30)$$

Expanding to first order in the quantities v and g, we obtain $\gamma \approx -(v - |g|)/\pi v_F$, which coincides with the perturbative result from the $g_2^{(2)}$ term at the r.h.s. of equation (28). This term is to be replaced now by the full nonperturbative result. On the other hand, we take for $g_1^{(1)}$ and $g_2^{(1)}$ the same strength, equal in absolute value to $|g|$, relying on the fact that the energy of the phonons exchanged with momentum $2k_F$ becomes comparable to the energy of the optical phonons near zero momentum. According to the selection rule (7) for the electron-phonon couplings in the armchair nanotubes, the last term proportional to $g_1^{(2)}$ is absent in the undoped nanotubes, since it stands for processes in which the electrons shift from one Fermi point to the other, with exchange also of the two subbands. Then, the improved scaling equation of the response function for s-wave order parameter becomes

$$E_c \frac{\partial \log \overline{R}(\omega)}{\partial E_c} = \frac{1}{2} - \frac{1}{2}\sqrt{1 - 4|g|/\pi v_F} + \frac{1}{2n} - \frac{1}{2n}\sqrt{1 + 4nv/\pi v_F} + \frac{1}{\pi v_F} 2|g|. \quad (31)$$

When dealing with doped armchair nanotubes, the only difference in the evaluation of $\overline{R}(\omega)$ is that the contribution from $g_1^{(2)}$ to the r.h.s. of (31) is nonvanishing, since the selection rule (7) does not constrain that coupling away from half-filling. Its contribution has attractive character, and it can be taken equal to $|g|$ in absolute value, when the system is suitably doped. Then, the only change in equation (31) is that the last term becomes $3|g|/\pi v_F$ in the case of the doped armchair nanotubes.

From the scaling equation for the response function, we can determine the regimes in which the superconducting correlations grow large at low energies in the nanotube ropes. We observe that, for positive values of the total anomalous dimension at the r.h.s. of (31), the response function $\overline{R}(\omega)$ has a power-law divergence for increasing values of the cutoff E_c. On dimensional grounds, the dependence of $\overline{R}(\omega)$ on the frequency ω must come through the ratio ω/E_c. Thus, the superconducting correlations are triggered at low energies for positive values of the anomalous dimension. We have represented in Figure 3 the region

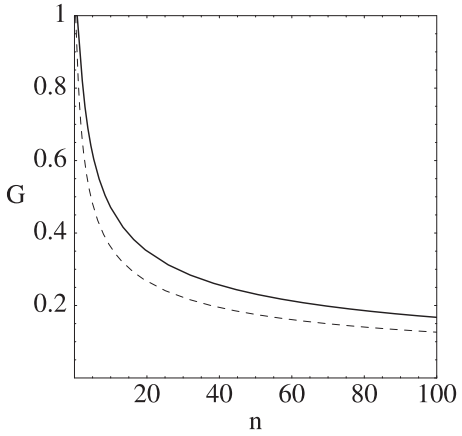

Fig. 3. Phase diagram of armchair nanotubes given in terms of the effective coupling of the attractive interaction $G = 4|g|/\pi v_F$ and the number n of metallic nanotubes in a rope. The full (dashed) line represents the boundary between the lower nonsuperconducting phase and the upper phase where superconducting correlations grow large at low energies in the undoped (doped) nanotubes.

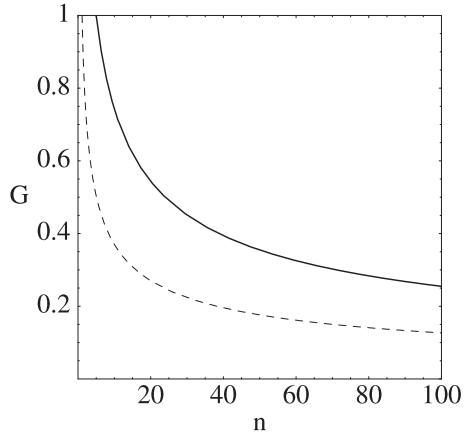

Fig. 4. Phase diagram of zigzag nanotubes given in terms of the effective coupling of the attractive interaction $G = 4|g|/\pi v_F$ and the number n of metallic nanotubes in a rope. The full (dashed) line represents the boundary between the lower nonsuperconducting phase and the upper phase where superconducting correlations grow large at low energies in the undoped (doped) nanotubes.

where this happens, in the phase diagram drawn in terms of the strength $|g|$ of the effective attractive interaction and the number n of metallic nanotubes in the rope. We notice the slightly greater extension of the superconducting regime in the doped armchair nanotubes.

Turning to the case of the undoped zigzag nanotubes, we recall that the selection rules (10) on the electron-phonon couplings imply then the absence of forward-scattering interactions mediated by phonons. We can improve again the perturbative equation (28) by including the exact contribution to the anomalous dimension from the forward-scattering processes mediated by the Coulomb interaction. We end up in this way with the scaling equation

$$E_c \frac{\partial \log \overline{R}(\omega)}{\partial E_c} = \frac{1}{2n} - \frac{1}{2n}\sqrt{1 + 4nv/\pi v_F} + \frac{1}{\pi v_F} 2|g|. \quad (32)$$

We have taken into account that the contribution from $g_1^{(2)}$ vanishes now due to the selection rule (10), since that coupling stands for processes with no exchange of subbands in the present geometry.

In the case of the zigzag nanotubes, doping the system leads to a most significant change, since it opens a number of scattering processes by phonon exchange that were forbidden at half-filling. The Hamiltonian for the forward-scattering interactions in the doped zigzag nanotubes is given by (23). By means of a computation similar to that in reference [18], one obtains that the contribution from those interactions to the anomalous dimension of the Cooper pair propagator is now

$$\gamma = \frac{1}{2} - \frac{n-1}{2n}\sqrt{1 - 4|g|/\pi v_F} - \frac{1}{2n}\sqrt{1 + 4nv/\pi v_F - 4|g|/\pi v_F}. \quad (33)$$

The perturbative expansion of this expression gives $\gamma \approx -(v - |g|)/\pi v_F$, to the first order in v and g. This approximation coincides again with the perturbative contribution from $g_2^{(2)}$ to the scaling equation (28). This can be now improved nonperturbatively by including the exact contribution from the forward-scattering interactions in the doped zigzag nanotubes:

$$E_c \frac{\partial \log \overline{R}(\omega)}{\partial E_c} = \frac{1}{2} - \frac{n-1}{2n}\sqrt{1 - 4|g|/\pi v_F} - \frac{1}{2n}\sqrt{1 + 4nv/\pi v_F - 4|g|/\pi v_F} + \frac{1}{\pi v_F} 3|g|. \quad (34)$$

We discern the regimes where the superconducting correlations grow large in the zigzag nanotubes by identifying the points in the respective phase diagrams where the r.h.s. of (32) or (34) become positive. This leads to the boundaries that have been represented in Figure 4 for the cases of undoped and doped zigzag nanotubes. The regions where the response function diverges at low energies correspond to the phases placed above the respective boundary lines. We observe that, as expected, the phase of superconductivity has a sensibly smaller extension in the case of the undoped zigzag nanotubes.

5 Conclusions

In this paper we have incorporated an exact treatment of the long-range Coulomb interaction, leading to the nonperturbative evaluation of its effects in the nanotube ropes. Thus, we have shown that the substantial reduction of the Coulomb repulsion due to the electrostatic coupling between metallic nanotubes is a sensible effect, that should

be measured specially in thick ropes. Looking at the phase diagrams in Figures 3 and 4, we observe the general trend that leads to the onset of the superconducting correlations at sufficiently large values of n. The existence of the boundary for the regime of superconductivity should be confirmed experimentally through the dependence of the transport properties on the content of metallic nanotubes in the ropes.

Regarding the effective attractive interaction, we have made a nonperturbative description of the forward-scattering processes mediated by phonons, while the rest of the processes have been considered at a perturbative level. This means that the map of the different regions in the phase diagrams can only be trusted away from the upper limit $4|g|/\pi v_F = 1$. This precludes, in particular, the elucidation of the existence of superconducting correlations in individual carbon nanotubes, for large values of the strength $|g|$ of the attractive interaction. On the other hand, the effective attractive interaction is in the weak-coupling regime for the nanotubes found typically in a rope. The order of magnitude of $|g|$ depends on the nanotube radius and, for the average value $R \approx 0.7$ nm in the ropes, it turns out that $|g| \sim 0.1 v_F$. Although the phonon-mediated interaction is renormalized at low energies, it can be shown that the scaling of the different couplings is very smooth and that the perturbative approach remains reliable down to temperatures well below 1 K [37].

The phase diagrams shown in Figures 3 and 4 reflect the different strength of the superconducting correlations depending on the geometry of the nanotubes and on whether they are doped or not. This investigation extends the results from previous studies, which have focused on the consideration of forward-scattering processes in armchair nanotubes [18]. We conclude that the case of the undoped zigzag nanotubes is extreme in that the phase with superconducting correlations has the smallest extension in the phase diagram. This should not affect much the transport properties of the ropes, which contain nanotubes with all kind of helicities, but it is a feature to be considered when dealing with individual nanotubes. In general, we have to expect a phase diagram evolving from that in Figure 3 to the phase diagram in Figure 4, for nanotubes with different chiral angles interpolating between armchair and zigzag geometries.

In the experiments where superconducting correlations have been measured, genuine superconducting transitions have been observed in ropes with a content of about 100 metallic nanotubes [14]. In the exhaustive report presented in reference [13], one can see that the transition is not completed in some cases, in particular in a 1 μm-long rope made of a total of about 45 nanotubes. This observation is consistent with the form of the phase diagrams represented in Figures 3 and 4. Given that a superconducting transition has been observed in another 1 μm-long rope mounted on the same kind of electrodes [13], the absence of transition in the thinner rope can be related to the failure of the superconducting correlations to grow due to the Coulomb repulsion. The thin rope, with a content of about 15 metallic nanotubes, should correspond to a point in the phase diagram outside the superconducting regime. From inspection of the diagrams in Figures 3 and 4, that would imply a value of the effective coupling $4|g|/\pi v_F$ below 0.3, for the nanotubes found typically in a rope.

Although we have not discussed the conditions that make possible the three-dimensional Cooper-pair coherence in the rope, it is not difficult to see that such an effect goes along with the growth of the superconducting correlations in each metallic nanotube. This comes from the fact that the same combination of couplings appearing at the r.h.s. of equation (28) drives also the behavior of the Cooper-pair tunneling amplitude between neighboring metallic nanotubes in the rope [18]. Thus, the same condition used to determine the onset of superconducting correlations in each nanotube applies also to establish the coherence of the Cooper pairs in the transverse directions of the rope. This clarifies the character of the phases at the two sides of the boundaries drawn in Figures 3 and 4. These boundaries mark also the points where the coherence of the Cooper pairs is lost from the three-dimensional point of view. The region below each boundary corresponds therefore to a metallic phase of the nanotubes, down to temperatures comparable to those of the transitions reported in reference [13]. The stability of these metallic phases is only perturbed by the scaling of the phonon-mediated interactions to strong-coupling, but this happens in general at much lower temperatures, when nonperturbative effects may involve the breakdown of the homogeneous description of the system [37].

References

1. R. Saito, M. Fujita, G. Dresselhaus, M.S. Dresselhaus, Appl. Phys. Lett. **60**, 2204 (1992)
2. J.W. Mintmire, B.I. Dunlap, C.T. White, Phys. Rev. Lett. **68**, 631 (1992)
3. N. Hamada, S. Sawada, A. Oshiyama, Phys. Rev. Lett. **68**, 1579 (1992)
4. R. Egger, A.O. Gogolin, Phys. Rev. Lett. **79**, 5082 (1997); Eur. Phys. J. B **3**, 281 (1998)
5. C. Kane, L. Balents, M.P.A. Fisher, Phys. Rev. Lett. **79**, 5086 (1997)
6. M. Bockrath, D.H. Cobden, J. Lu, A.G. Rinzler, R.E. Smalley, L. Balents, P.L. McEuen, Nature **397**, 598 (1999)
7. Z. Yao, H.W. Ch. Postma, L. Balents, C. Dekker, Nature **402**, 273 (1999)
8. M. Bockrath, D.H. Cobden, P.L. McEuen, N.G. Chopra, A. Zettl, A. Thess, R.E. Smalley, Science **275**, 1922 (1997)
9. S.J. Tans, M.H. Devoret, H. Dai, A. Thess, R.E. Smalley, L.J. Geerligs, C. Dekker, Nature **386**, 474 (1997)
10. S. Frank, P. Poncharal, Z.L. Wang, W.A. de Heer, Science **280**, 1744 (1998)
11. W. Liang, M. Bockrath, D. Bozovic, J.H. Hafner, M. Tinkham, H. Park, Nature **411**, 665 (2001)
12. A.Yu. Kasumov, R. Deblock, M. Kociak, B. Reulet, H. Bouchiat, I.I. Khodos, Yu.B. Gorbatov, V.T. Volkov, C. Journet, M. Burghard, Science **284**, 1508 (1999)

13. A.Yu. Kasumov, M. Kociak, M. Ferrier, R. Deblock, S. Guéron, B. Reulet, I.I. Khodos, O. Stéphan, H. Bouchiat, report `cond-mat/0307260`, to be published in Phys. Rev. B
14. M. Kociak, A.Yu. Kasumov, S. Guéron, B. Reulet, I.I. Khodos, Yu.B. Gorbatov, V.T. Volkov, L. Vaccarini, H. Bouchiat, Phys. Rev. Lett. **86**, 2416 (2001)
15. Z.K. Tang, L. Zhang, N. Wang, X.X. Zhang, G.H. Wen, G.D. Li, J.N. Wang, C.T. Chan, P. Sheng, Science **292**, 2462 (2001)
16. J. González, Phys. Rev. Lett. **87**, 136401 (2001)
17. J. González, Phys. Rev. Lett. **88**, 076403 (2002)
18. J. González, Phys. Rev. B **67**, 014528 (2003)
19. L.G. Caron, C. Bourbonnais, Phys. Rev. B **29**, 4230 (1984)
20. H. Suzuura, T. Ando, Phys. Rev. B **65**, 235412 (2002).
21. D. Loss, T. Martin, Phys. Rev. B **50**, 12160 (1994)
22. A. De Martino, R. Egger, Phys. Rev. B **67**, 235418 (2003)
23. D. Sánchez-Portal, E. Artacho, J.M. Soler, A. Rubio, P. Ordejón, Phys. Rev. B **59**, 12678 (1999)
24. L.M. Woods, G.D. Mahan, Phys. Rev. B **61**, 10651 (2000)
25. R. Saito, A. Jorio, A.G. Souza Filho, G. Dresselhaus, M.S. Dresselhaus, M.A. Pimenta, Phys. Rev. Lett. **88**, 027401 (2002)
26. J. González, F. Guinea, M.A.H. Vozmediano, Nucl. Phys. B **406**, 771 (1993)
27. L. Pietronero, S. Strässler, H.R. Zeller, M.J. Rice, Phys. Rev. B **22**, 904 (1980)
28. R.A. Jishi, M.S. Dresselhaus, G. Dresselhaus, Phys. Rev. B **48**, 11385 (1993)
29. D.W. Wang, A.J. Millis, S. Das Sarma, Phys. Rev. B **64**, 193 307 (2001)
30. R. Egger, H. Grabert, Phys. Rev. Lett. **79**, 3463 (1997)
31. S. Bellucci, J. González, Eur. Phys. J. B **18**, 3 (2000)
32. A.A. Maarouf, C.L. Kane, E.J. Mele, Phys. Rev. B **61**, 11156 (2000)
33. H. Stahl, J. Appenzeller, R. Martel, Ph. Avouris, B. Lengeler, Phys. Rev. Lett. **85**, 5186 (2000)
34. J. Sólyom, Adv. Phys. **28**, 201 (1979)
35. H.J. Schulz, in *Correlated Electron Systems*, Vol. 9, edited by V.J. Emery (World Scientific, Singapore, 1993)
36. Yu.A. Krotov, D.-H. Lee, S.G. Louie, Phys. Rev. Lett. **78**, 4245 (1997)
37. J.V. Alvarez, J. González, Phys. Rev. Lett. **91**, 076401 (2003)